March 1, 1981

Radar interferometry: A new technique for studyingplasma turbulence in the ionosphere

D. T. Farley
H. M. Ierkic
Bela G. Fejer, *Utah State University*

JOURNAL OF GEOPHYSICAL RESEARCH, VOL. 86, NO. A3, PAGES 1467-1472, MARCH 1, 1981

Radar Interferometry: A New Technique for Studying Plasma Turbulence in the Ionosphere

D. T. FARLEY, H. M. IERKIC, AND B. G. FEJER

School of Electrical Engineering, Cornell University, Ithaca, New York 14853

A new radar interferometer technique has been developed and used successfully at the Jicamarca Radio Observatory in Peru to study the strong nighttime plasma turbulence in the equatorial electrojet. The technique represents a major step forward in radar probing of turbulent irregularities such as (but not limited to) those in the electrojet. In many situations it provides far more information than previous Doppler measurements. We form the cross spectrum of the backscattered signals received from approximately overhead on two antennas, separated in this case along an east-west baseline, as well as the individual power spectra. From the phase of the cross spectrum at different Doppler frequencies we can determine the individual positions of plasma wave packets propagating vertically with different velocities, and we find, for example, that oppositely propagating waves always come from distinctly separated regions. The data allow us to study the eddy structure within the electrojet in far more detail than hitherto possible, and by using the irregularity patches as tracers and following their east-west motion, we can obtain a vertical profile of drift velocity. Our first observations of this sort have shown that at night the vertical Doppler velocity at times may substantially exceed the mean horizontal velocity of the patch and the small horizontal velocity near the top and bottom of the layer may actually be westward when the main motion is eastward.

INTRODUCTION

This paper describes an important new radar scattering technique developed at Jicamarca for studying two-dimensional ionospheric plasma turbulence and presents some of the first results obtained from investigations of the equatorial electrojet. More detailed discussion of observations of the irregularities in the electrojet and in the equatorial *F* region will be given in subsequent publications.

The technique is an extension of a method described by *Woodman* [1971], who showed that a radar interferometer could accurately determine the position of a highly localized scattering region. Using the north and south quarters of the large 50-MHz, vertically pointing array at Jicamarca, he was able to measure very precisely the locus of points in the *F* region at which the line of sight from the radar was perpendicular to the magnetic field, since the scattering irregularities are highly field aligned. He showed that the inclination angles of the then existing magnetic field models were in error by roughly 1°.

The technique we shall describe here is similar, except that the baseline is east-west and we also make use of the spectral information in the scattered signal. The method works when the scattering region is highly structured, or more specifically, when the received scattered signal within a particular small interval of Doppler shift corresponds to a small range of angular positions within the scattering volume. We transmit using the entire Jicamarca array (48 $\lambda \times 48\ \lambda$), pointed approximately vertically and perpendicular to the magnetic field, and receive separately on the east and west quarters. Each signal is sampled at a number of ranges and then later Fourier-transformed. Next we compute the normalized cross spectrum of the two signals for each range and average the results. For each frequency (Doppler shift) the magnitude of the cross spectrum is a measure of the localization in the E-W plane of the corresponding echoing center (point targets correspond to a value of unity) and the phase determines the mean angular position in the E-W plane. In essence we cross correlate the two signals one frequency at a time, since each frequency (Doppler shift) is presumed to correspond to a particular plasma wave at a different location. In *Woodman*'s [1971] measurements the signal voltages were cross-correlated directly, since the entire signal came from the same location (the point of perpendicularity) in the meridional plane. Whenever the scattered signal is diffuse and signals with the same Doppler shift come from many regions throughout the scattering volume, the interferometer technique fails.

Our first observations were made during the night, when the electrojet is highly structured, and the results exceeded our expectations. We found that at least a portion of the echo at this time usually does indeed come from a few (1–3 typically) discrete locations, even when most of the echo is diffuse. Furthermore, the east-west motion of the discrete echoing centers through the scattering volume can be tracked. We thus can determine some characteristics of the large eddies in which the short-wavelength irregularities are imbedded and can also obtain profiles of drift velocity as a function of altitude and time, using the irregularities as tracers and assuming that they move with the background plasma. These results add new information to that obtained in our most recent previous study of the nighttime turbulence [*Farley et al.*, 1978]. The general properties and current theories of the electrojet instabilities are discussed in reviews by *Farley* [1979], *Fejer* [1979], and *Fejer and Kelley* [1980]. Further details concerning some of the material presented here are given by *Ierkic* [1980].

THE INTERFEROMETER TECHNIQUE

The geometry of the experiment is illustrated in Figure 1. Suppose to begin with that there is only a single small clump of elementary scatterers within a particular range interval in the scattering volume (defined by the antenna beam and pulse length). These are elongated along the magnetic field, are moving with a radial velocity of $\omega\lambda_0/4\pi$ (λ_0 is the radar wavelength) towards the radar, and finally are located at a mean angular position $\bar{\theta}_\omega$ in the east-west plane. We transmit using the whole antenna, thereby restricting the region probed to about one lobe of the interferometer pattern with the geome-

Paper number 80A1364.
0148-0227/81/080A-1364$01.00

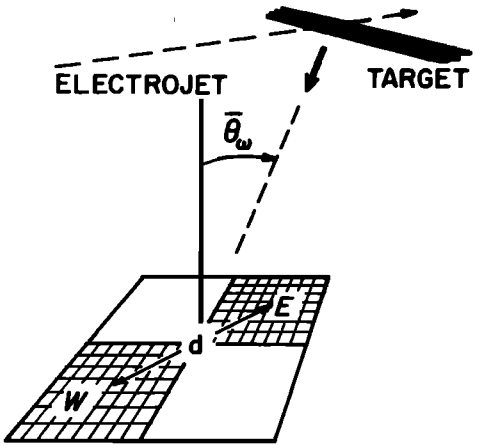

Fig. 1. The geometry of the electrojet interferometer. The entire Jicamarca 50-MHz array was used for transmission, but the scattered signals were received separately on the east and west quarters, whose phase centers are separated by the distance d which is 208.2 m. The field-aligned 'target' is assumed to occupy a small range of angles centered about the small mean angle $\bar{\theta}_\omega$, and the subscript ω refers to the Doppler shift of the echo.

try as shown, and receive separately on the east and west quarters, whose phase centers are a distance d apart. The signal voltage from the east quarter, say, can be written as

$$V_E(t) = \sum_j A_j(\omega) \exp(i\phi_j + i\omega t) \tag{1}$$

where ϕ_j is a random phase angle, uniformly distributed in the interval $[0, 2\pi]$, that corresponds to a particular elemental scatterer, and A_j is the corresponding amplitude. After Fourier-transforming a relatively short segment of data we have

$$V_E(\omega) = \sum_j A_j(\omega) \exp(i\phi_j) \tag{2}$$

where the time variation of $A(\omega)$ is assumed to be slow. Similarly, for the signal from the west antenna,

$$V_W(\omega) = g \sum_j A_j(\omega) \exp(i\phi_j - ikd\theta_j) \tag{3}$$

where k is $2\pi/\lambda_0$ and we have replaced $\sin\theta_j$ with θ_j, the angular position of the jth scatterer, since in practice, the angles of interest are small. The factor g represents a possible gain difference, but the gains will soon drop out of the calculations.

Since the ϕ_j are independent of each other and uniformly distributed over $[0, 2\pi]$, taking ensemble averages (equivalent to temporal or spatial averages) leads to the following results:

$$\langle e^{i\phi_j} \rangle = 0 \tag{4}$$

$$\langle V_E(\omega) V_W^*(\omega) \rangle = \left(g \sum_j A_j^2 \right) \langle e^{ikd\theta_j} \rangle \tag{5}$$

Finally, defining the complex normalized cross spectrum $S_{EW}(\omega)$ by

$$S_{EW}(\omega) = \frac{\langle V_E(\omega) V_W^*(\omega) \rangle}{\langle |V_E(\omega)|^2 \rangle^{1/2} \langle |V_W(\omega)|^2 \rangle^{1/2}} \tag{6}$$

we obtain

$$S_{EW}(\omega) = \langle e^{ikd\theta_j} \rangle \tag{7}$$

If we now assume for convenience that the θ_j have a Gaussian distribution with mean $\bar{\theta}_\omega$ and variance σ_ω^2, (7) reduces to

$$S_{EW}(\omega) = e^{ikd\bar{\theta}_\omega} \exp(-\tfrac{1}{2}k^2 d^2 \sigma_\omega^2) \tag{8}$$

Any other reasonable distribution for θ_j (e.g., uniform over a small interval) would give a similar result.

It should be fairly obvious that we can easily generalize the above to the case where there are several scattering regions, each with its own (different) Doppler shift ω, mean position $\bar{\theta}_\omega$, and angular spread σ_ω. Adding the extra scatterers will simply cause (8) to be replaced by a summation over the Doppler shifts.

It is worth emphasizing that S_{EW} is normalized frequency by frequency, and so, as we shall see, frequencies for which the individual power spectra $|V(\omega)|^2$ are weak may have large

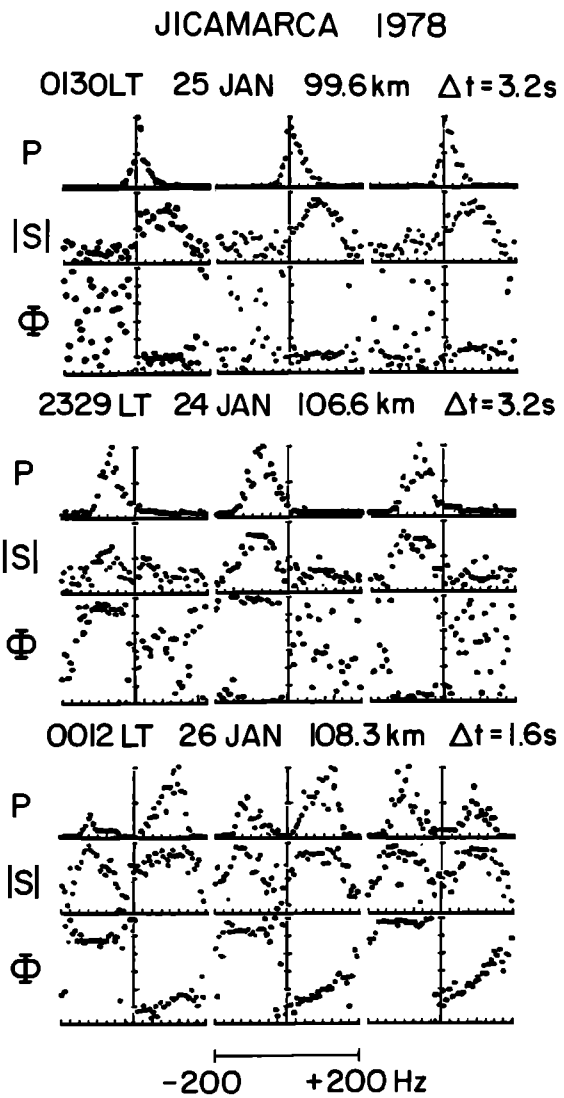

Fig. 2. Examples of data obtained from the interferometer. The rows labeled P are the normalized power spectra from one receiver, the rows labeled $|S|$ are the magnitude of the normalized cross spectrum S_{EW} defined in (8) of the text and referred to as the coherency, and the rows labeled Φ are the phase angles of the cross spectrum. (Top) Data from relatively weak echoes near the bottom of the echoing region; (middle) fairly strong type 2 echoes; (bottom) type 1 echoes of opposite Doppler shifts which come from different locations within the scattering volume. A Doppler shift of +100 Hz represents a downward phase velocity of 300 m/s.

normalized cross spectra (if these weak signals come from a single small location), and vice versa (if signals within the same quantized interval of Doppler shift come from a broad region or several different regions within the scattering volume). Random cosmic or receiver noise gives a small cross spectrum, of course, not because it is weak, but because there is no phase relationship between the two signals. However, when the large Jicamarca radar is used for electrojet measurements, even the relatively weakest components of the scattered signal are often far above the noise level.

The full array at Jicamarca has a half-power beam width of about 1° (about 2° between 10-dB points in the E-W direction). Hence the scattering volume occupies 1–2 km in the E-W direction at electrojet altitudes of about 105 km and proportionally more at F region altitudes. From (8) we can relate the phase of the cross spectrum to the angle $\bar{\theta}_\omega$ and then to an east-west position (for an east-west baseline), which will depend on altitude. At an altitude h, the separation δx corresponding to a phase difference $\delta\phi$ (radians) is simply

$$\delta x = h\delta\phi/kd \tag{9}$$

For the present measurements at Jicamarca the spacing d was 34.65 λ_0, and so (9) becomes

$$\delta x = 4.593 \times 10^{-3} h\delta\phi \tag{10}$$

At an altitude of 105 km, for example, a phase increase of 10° corresponds to an eastward displacement of 84.2 m. The peak transmitted power was about 1 MW for the experiments we shall discuss, and the pulse length was 10 μs with a matched receiver bandwidth. Eight altitudes from 97.8 to 110.1 km, and separated by 1.75 km, were sampled at a sampling rate (pulse repetition frequency) of 400 Hz. The signal voltages were mixed to baseline (the 50-MHz carrier frequency was removed), and the resulting voltages from the two quadrature channels of the two receivers were digitized and stored on tape for the off-line spectral analysis.

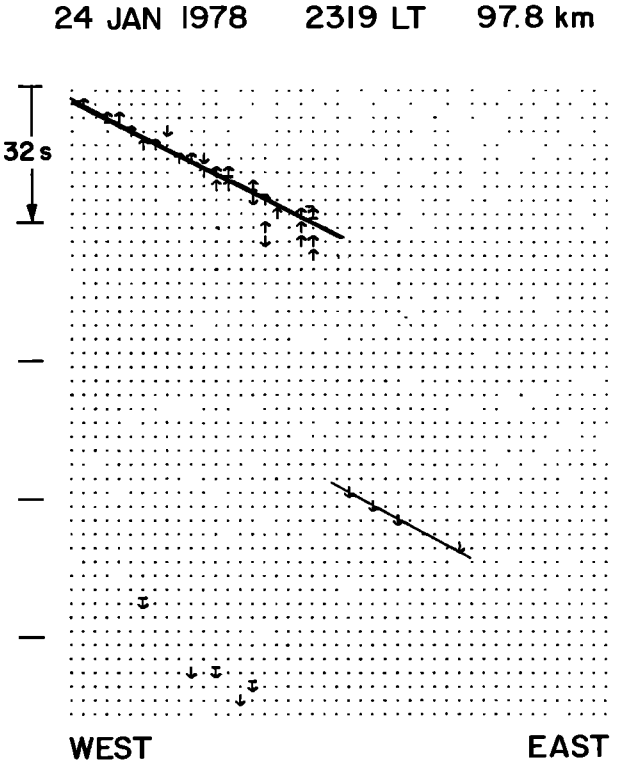

Fig. 3. Data showing a slow (~30 m/s) eastward drift. The grid points are separated in phase by 8° (or 62.7 m in the east-west direction at the altitude of 97.8 km) and in time by 3.2 s, with time progressing downwards. The local time of 2319 is the approximate starting time. An arrow indicates an echo with high coherency, the arrow points in the direction of the vertical phase velocity of the scattering plasma wave, and a tail on the arrow means the magnitude of the Doppler shift was ≥100 Hz.

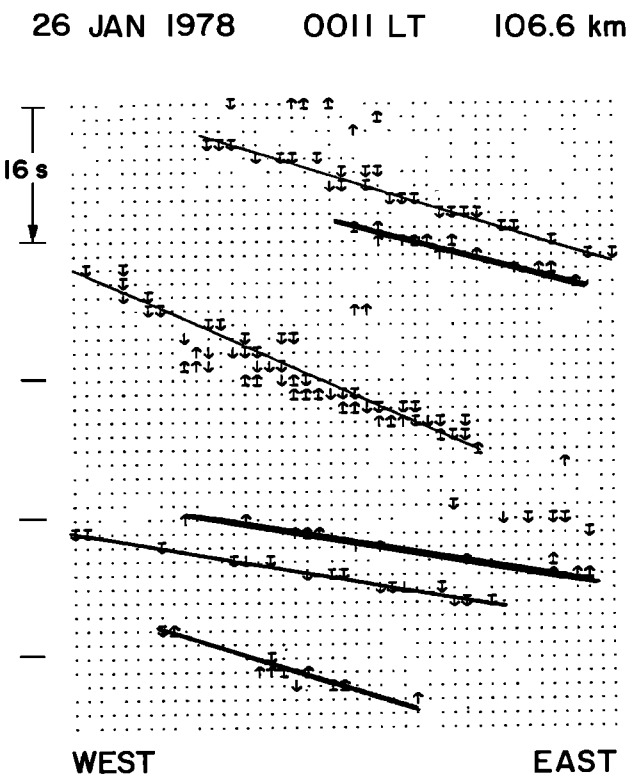

Fig. 4. Data similar to those in Figure 3 but showing more structure and a higher eastward velocity (>100 m/s). Note the different time scale.

The first step in the analysis was to calculate a 64-point complex FFT of each signal, implying a frequency interval of 400/64 = 6.25 Hz. The cross product and normalizing terms in (6) were then calculated, and the process was repeated to give a 1.6- or 3.2-s average of the data (10 or 20 spectral samples, respectively) before S_{EW} was computed. These short integrations were chosen so that we could follow the sometimes rapid changes in phase that occurred as the irregularities moved through the antenna beam. The price one pays for this good time resolution is rather large statistical errors in the spectral estimates. As we shall see, however, useful results can be obtained in spite of these statistical uncertainties.

OBSERVATIONS AND DISCUSSION

The data to be presented were gathered around midnight on two nights in January 1978. The radar was pointed approximately vertically and perpendicular to the magnetic field. For each of the eight altitudes sampled and for each time period of 1.6 or 3.2 s, we calculated the power spectrum from each arm of the interferometer and the amplitude and phase of the normalized cross spectrum S_{EW}. Figure 2 shows three representative short sets of samples of the results. In each set the top row labeled P is the normalized power spectrum from the

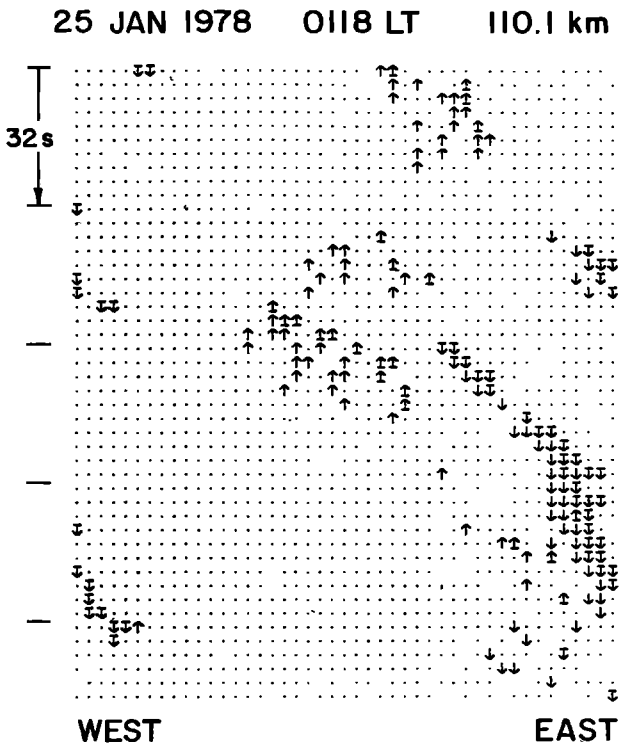

Fig. 5. Data showing weak disordered motion from near the top of the echoing region.

west antenna (the results from the east antenna were the same except for statistical differences), i.e., $|V_W(\omega)|^2$ was normalized to give a maximum value of unity. The second row shows the amplitude $|S_{EW}(\omega)|$ of the cross spectrum (often called the coherency), and the third row, labeled Φ, gives the phase angle arc $[S_{EW}(\omega)]$. The cross spectra are normalized as in (6), and the phase angle covers 2π radians (each tick mark on the vertical axis is 60°). The samples in the top two sections were integrated for 3.2 s and are separated by the same amount, with time increasing to the right, while for the last sample the integration time and interval was reduced to 1.6 s. An increase in phase angle corresponds to a displacement of the echoing region to the east; for an altitude of 100 km, for example, 60° corresponds to 481 m. In these preliminary measurements no absolute calibration of the phase shifts through the entire system was made, and so we cannot assign a precise position to each phase angle; only the changes are significant. The Doppler frequencies cover the range ±200 Hz, and positive values correspond to downgoing plasma waves.

The first (top) set of data in Figure 2 is from the bottom part of the electrojet and shows a typical [*Balsley and Farley*, 1973; *Fejer et al.*, 1976] narrow power spectrum centered near zero Doppler shift. Note that the coherency for this data set (the second row of the figure) does not maximize near zero Doppler, however, but rather in the vicinity of +75 Hz, corresponding to a downward velocity of 225 m/s, a frequency at which the power spectrum appears almost to vanish. Actually, the signal at this Doppler shift is still far above the noise level; it appears small in the plot only because of the normalization by the much stronger signals near zero Doppler. These results imply that the signal near zero Doppler is diffuse, coming from many locations within the scattering volume (σ_ω^2 in (7) is large), whereas the highly shifted components come from a localized (coherent) region. Looking at the third row, the phase angle of the cross spectra, we see that the points are highly organized for frequencies where the coherency is large but are nearly randomly distributed at other frequencies. Moreover, there is a small but perceptible increase in the phase in the 6.4 s between the first and third samples, implying an eastward motion of the position of the localized echoing region.

The second data set in Figure 2 illustrates an upward going wave with a mean velocity of about 200 m/s at an altitude near the center of the electrojet. In this case the power spectra and coherency maximize at about the same frequency, and again the corresponding phase angles increase significantly in 6.4 s (note that the angles 'wrap around' and reappear at the bottom of the right-hand panel).

The last set of data, from 26 January and 108 km, shows a particularly interesting sequence. In spite of the short (1.6 s) integrations the power spectra clearly show type 1 peaks corresponding to both upgoing and downgoing waves with velocities of the order of the ion acoustic velocity, and the cross spectral coherency is nearly unity for both, independent of the relative amplitudes in the power spectra. There are several significant points to notice in the phase angle data for this case. First of all, the angles are distinctly different for the two spectral regions, implying that the upgoing and downgoing plasma waves are in different locations within the scattering volume; the multiple peaks in the power spectra result from spatial averaging. This result is just what we would expect if the vertical velocities are due to convection within large scale 'whirls' or eddies in the plane perpendicular to the magnetic field [*Farley and Balsley*, 1973; *Sudan et al.*, 1973], but this is the first direct confirmation of such behavior. Secondly, we see that both the upgoing and downgoing scattering centers are being convected eastward, as in the previous two cases, but the velocity is considerably higher; the phase change is roughly 60° (more than 500 m at the altitude in question) in

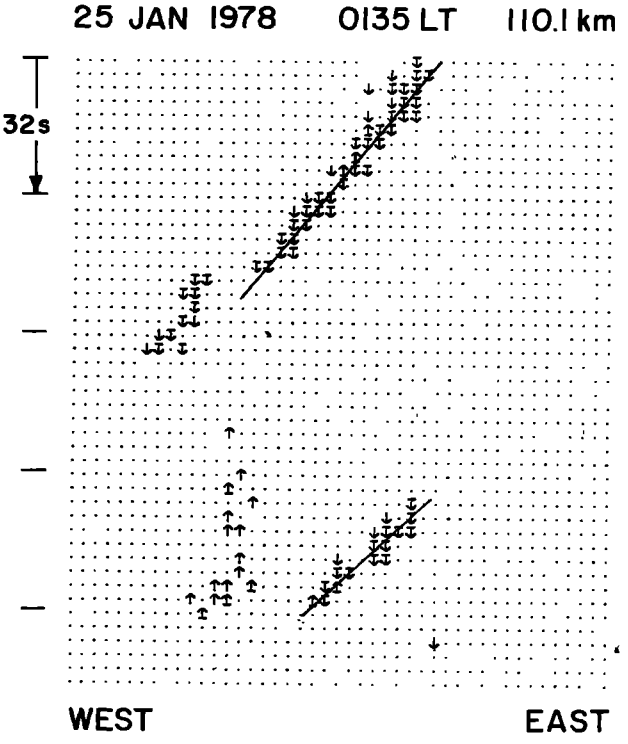

Fig. 6. Data showing slow westward motion from the same altitude and from shortly after the observations shown in Figure 5.

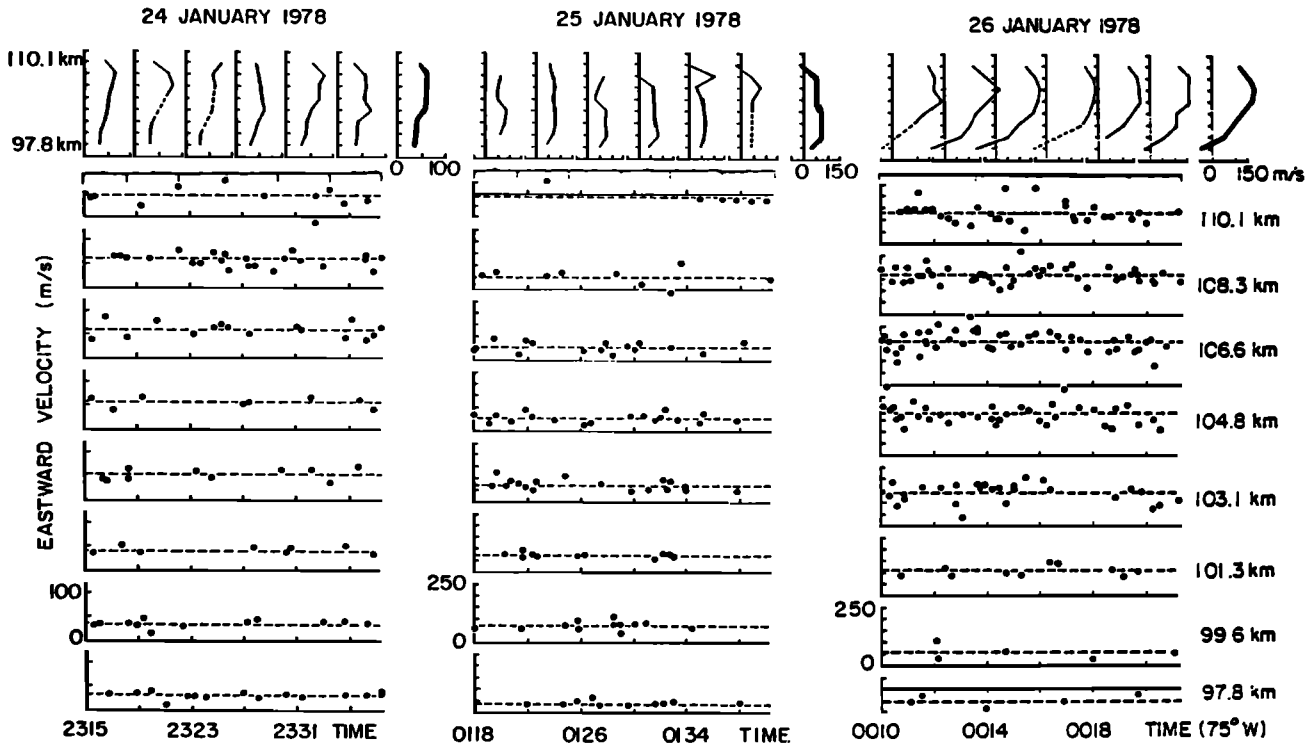

Fig. 7. Velocity data obtained from the slopes of lines such as those shown in Figures 3–6.

only 3.2 s. Finally, note the slope in the curve of phase versus frequency for the positive Doppler shifts, with the highest velocities coming from the most easterly locations, but the absence of any such slope for the negative shifts. We have not yet done a careful study of this effect, but our preliminary observations suggest that there probably is a real asymmetry, even though the effect is sometimes observed for negative Dopplers. The downgoing waves are also more common at night, although that is not obvious from our figures here, an asymmetry which has been noted before [*Farley et al.*, 1978] and which is the opposite of the daytime asymmetry [*Fejer et al.*, 1976].

The slope in the cross-spectral phase curve should tell us something about the large-scale eddy motion. For example, some sort of quasi-cycloidal flow towards the east and clockwise (looking north) would tend to have the largest downward velocities at the most easterly locations. We need to study this aspect of the data further, however, before proposing any detailed model.

It is clearly not practical to display hours or even minutes worth of data in the format of Figure 2. The presentations in Figures 3–6 illustrate one way to begin to compress the data. To obtain these figures, we parameterize data such as those in Figure 2 as follows: (1) The 64 frequencies are divided into 16 blocks of 4. (2) If the coherency of at least 2 of the 4 frequencies in a particular block is 0.7 or greater, the phases of the 4 are averaged and quantized to the nearest 8° step. (3) The result is plotted on the appropriate grid location in the E-W direction in Figures 3–6 as an arrow pointed up (down) for negative (positive) Doppler frequencies and with (without) a tail for the 8 frequency blocks farthest from (nearest to) zero (if several frequency blocks have the same phase, only one arrow will show). (4) This process is repeated for every time interval (separated by the integration times of 1.6 or 3.2 s for these data), with time progressing downwards in the figures.

As an aid to the eye we have drawn heavy (light) straight lines through groups of upward (downward) pointing arrows which seem to have an obvious identity. The slopes of these lines give the horizontal component of the apparent velocity of the echoing centers, and in the absence of evidence to the contrary, we will assume that these centers are being convected within the large-scale eddies.

Figure 3 shows an example of slow eastward drift near the bottom of the electrojet. Figure 4, from near the central portion, shows a much more rapid drift (note the change in time scale) of about 150–250 m/s and much more structure. Note that except for a few very minor exceptions, the upward and downward pointing arrows are in distinct, spatially separated groups, in agreement with our discussion above of the bottom portion of Figure 2. Some groups of arrows maintain their identity while drifting a considerable distance. The first group of downward pointing arrows in Figure 4, for example, wraps around from the right-hand edge of the figure, reappears at the left, and continues to drift eastward for another 21 s before disappearing. The typical lifetime of these groups, tens of seconds, is comparable to earlier estimates made from Jicamarca data [*Farley and Balsley*, 1973; *Farley et al.*, 1978]. The typical distance between oppositely directed wave groups was always several hundred meters or more in these observations (the grid points in Figure 4 are separated by 68.4 m). There was also another, slower time scale, of the order of minutes, that was observed on plots (not shown here) of received power versus time and that presumably corresponds to still larger-scale (several kilometers or more) perturbations.

In Figure 5, from 110 km, the echoing regions continue to be in localized groups but do not show a clear drift pattern. A short time later at the same altitude (Figure 6) the drift velocity is clearly westward, although small, i.e., contrary to the velocity at lower altitudes which continues to be eastward.

Figures 3–6 still show only a small portion of the data. By

plotting all the observations from all altitudes and times in the format of Figures 3–6, measuring the drift velocities by drawing (by hand in this case) lines through obviously correlated groups of arrows, and plotting the results as a function of altitude and time, we obtain Figure 7, the final stage of data compression. Each point represents the slope of an individual line, the velocity profiles drawn with light lines represent about 4-min averages for January 24 and 25 but 2-min averages for January 26, and finally the three profiles drawn with heavy lines show the average of all the data in the respective periods. As noted above, the velocity is actually negative (westward) at the highest height observed on January 25 and the lowest height observed on January 26. This could be due to a westward wind or it could represent an actual reversal of the electric field. It is also important to note that the maximum mean eastward velocities observed on January 26 were no more than about 200 m/s, and yet vertically traveling type 1 waves with velocities greater than 300 m/s were prevalent during this period (see Figure 2). This result implies that the fluctuating horizontal electric field was often larger in magnitude than the mean vertical field, a conclusion which seems consistent with some rocket observations (M. C. Kelley, private communication, 1980) and theory [*Sudan et al.*, 1973].

CONCLUDING REMARKS

The radar interferometer measurements provide a powerful new tool for studying the equatorial plasma instabilities and resulting turbulence. In certain respects the technique provides a vast improvement in horizontal spatial resolution, compared to previous radar measurements at Jicamarca, and thereby permits studies of properties of the turbulence which were hitherto unobservable. Even the small amount of data described here has confirmed some of our earlier hypotheses (e.g., that echoes with positive and negative Doppler shifts come from different locations) and also posed new questions (e.g., what causes the slope sometimes observed on the cross-spectral phase plots?). We also seem to be able to measure the profile of horizontal drift velocity within the electrojet, at least at night. Attempts to make similar electrojet observations during daytime have so far been unsuccessful. Apparently, the daytime echoing regions are more uniformly distributed within the scattering volume, and consequently, the coherency is much lower than at night, even though the echoes are stronger because of the greater electron density.

In the near future we plan to improve both the altitude resolution and coverage of the electrojet measurements and to utilize the technique in the equatorial *F* region as well. The first exploratory *F* region observations were quite successful and will be described elsewhere. The interferometer technique should also prove very useful in future radar observations of auroral zone irregularities.

Acknowledgments. We are especially grateful to R. F. Woodman for his suggestion to us that interferometer measurements at Jicamarca might give interesting results, and we thank the Jicamarca staff for their help with the observations. This research was supported by the Atmospheric Sciences Division of the National Science Foundation through grant ATM78-12323. The Jicamarca Radio Observatory is operated by the Geophysical Institute of Peru, Ministry of Education, with support from the National Science Foundation and the National Aeronautics and Space Administration.

The Editor thanks C. L. Rino and R. A. Greenwald for their assistance in evaluating this paper.

REFERENCES

Balsley, B. B., and D. T. Farley, Radar observations of two dimensional turbulence in the equatorial electrojet, *J. Geophys. Res., 78,* 7174, 1973.

Farley, D. T., The ionospheric plasma, in *Solar System Plasma Physics,* edited by C. F. Kennel, L. J. Lanzerotti, and E. N. Parker, North-Holland, Amsterdam, 1979.

Farley, D. T., and B. B. Balsley, Instabilities in the equatorial electrojet, *J. Geophys. Res., 78,* 227, 1973.

Farley, D. T., B. G. Fejer, and B. B. Balsley, Radar observations of two dimensional turbulence in the equatorial electrojet, 3, Nighttime observations of type 1 waves, *J. Geophys. Res., 83,* 5625, 1978.

Fejer, B. G., and M. C. Kelley, Ionospheric irregularities, *Rev. Geophys. Space Phys., 18,* 401, 1980.

Fejer, B. G., D. T. Farley, B. B. Balsley, and R. F. Woodman, Radar observations of two dimensional turbulence in the equatorial electrojet, 2, *J. Geophys. Res., 81,* 130, 1976.

Fejer, J. A., Ionospheric instabilities and fine structure, *J. Atmos. Terr. Phys., 41,* 895, 1979.

Ierkic, H. M., Radar observations of the equatorial electrojet irregularities and theory of type 1 turbulence, Ph.D. thesis, Cornell Univ., Ithaca, N. Y., 1980.

Sudan, R. N., J. Akinrimisi, and D. T. Farley, Generation of small-scale irregularities in the equatorial electrojet, *J. Geophys. Res., 78,* 240, 1973.

Woodman, R. F., Inclination of the geomagnetic field measured by incoherent scatter, *J. Geophys. Res., 76,* 178, 1971.

(Received July 22, 1980;
revised September 22, 1980;
accepted September 24, 1980.)